Systematic Design of Wide-Bandwidth Photonic Crystal Waveguide Bends With High Transmission and Low Dispersion

Murtaza Askari, Babak Momeni, *Member, IEEE*, Mohammad Soltani, and Ali Adibi, *Senior Member, IEEE*

***Abstract*—We identify factors affecting transmission and dispersive properties of photonic crystal waveguide (PCW) bends, using 2-D simulations and present a method for systematic design of PCW bends to achieve high transmission and low dispersion over large bandwidths. The bends presented here have higher bandwidth and lower dispersion than bends already reported.**

***Index Terms*—Finite-difference time-domain (FDTD), integrated optics, photonic crystal (PC), waveguide bend.**

I. Introduction

TWO-DIMENSIONAL (2-D) planar photonic crystals (PCs) [1], [2] have attracted a lot of attention because of their unique characteristics for light propagation and ease of fabrication, using mature semiconductor fabrication techniques. Conventional 2-D planar PC structures are realized by etching a periodic array of air holes in a dielectric slab, e.g., silicon (Si). In these structures, photonic crystal waveguides (PCWs) are typically formed by adding a 1-D defect to the PC structure (e.g., by not etching a single row of air holes) [3], [4]. A unique feature of these PCWs is the existence of slow group velocity modes [5], [6], which does not occur in nonperiodic waveguides. These slow group velocity modes have numerous applications such as optical delay lines [7], [8] and for enhanced light-matter interaction [9], [10]. Bends are an integral part of an integrated optics platform; they allow compact integration of multiple optical functionalities in a single chip. The spatial extent of bends in a PCW is on the order of a lattice period. The lattice period in a PCW is of the order of the wavelength of light (inside the PC material), thus the size of bends in PCWs, is roughly on the order of the wavelength of light. The smaller bends in PCWs make these PCWs a promising candidate for compact integrated optical functionalities. An ideal bend must provide high transmission and low dispersion over a large bandwidth. Although dispersion is not a critical parameter in waveguides with continuous translation symmetry, it can be a limiting factor in application of waveguides with discrete translation symmetry, which are inherently dispersive. Extensive research has been carried out to design PCW bends with high transmission [11]–[14]. However, the dispersive behavior of PCW bends has largely been overlooked. Since PC structures are inherently dispersive, any design for bends in PCWs should consider their dispersive behavior, especially when wide bandwidth is required (e.g., in ultrafast optics) or in situations when an optical signal goes through a PCW bend multiple times (e.g., in a loop-based delay structure).

In this paper, we study PCW bends keeping both their transmission and dispersion behavior in view. We study the effect of air holes next to the bending region to identify factors that affect PCW bend performance and show how they can be engineered to achieve both high transmission and low dispersion over a large bandwidth. The design approach and the simulation platform used in this paper are introduced in Section II. The systematic design procedure and simulation results of our design are discussed in Section III. The performance of these bends is compared with that of the previously reported bends in Section IV. Final conclusions are made in Section V.

II. Design Philosophy and Simulation Platform

Different design methodologies have been used to design PCW bends. In one approach, the bend has been modeled as a cavity, and the design is based on tuning its resonance and field profile to achieve high transmission [11]. In another approach, the bend is modeled as an impedance-matching region, and the design is focused on optimizing it to achieve minimum reflection [12]. Both these techniques are inherently used for low-bandwidth matching, and these techniques do not result in a wide-bandwidth PCW bend due to narrowband nature of resonance or impedance matching. The PCW bend design technique proposed here, on the other hand, is based on mode matching [13], [15]. For the sake of clarity, we use triangular lattice PCWs as the platform. While this lattice is the most widely used platform, our approach can be easily extended to other 2-D PC lattices. In our approach, we model the PCW bend as a coupling region (CR) between two (Γ-J directed) waveguides [14], as shown in Fig. 1(a). The input light couples

Manuscript received November 26, 2009; revised February 24, 2010; accepted April 07, 2010. Date of publication April 22, 2010; date of current version May 26, 2010. This work was supported in part by the U.S. Air Force Office of Scientific Research through Dr. G. Pomrenke under Contract FA9550-07-1-0201.

M. Askari and A. Adibi are with the School of Electrical and Computer Engineering, Georgia Institute of Technology, Atlanta, GA 30332 USA (e-mail: murtaza.askari@gatech.edu; ali.adibi@ece.gatech.edu).

B. Momeni was with the School of Electrical and Computer Engineering, Georgia Institute of Technology, Atlanta, GA 30332 USA. He is now with the Basic Sciences Division, Fred Hutchinson Cancer Research Center, Seattle, WA 98109 USA.

M. Soltani was with the School of Electrical and Computer Engineering, Georgia Institute of Technology, Atlanta, GA 30332 USA. He is now with the Department of Physics and the Department of Electrical Engineering, Cornell University, Ithaca, NY 14853 USA (e-mail: ms2295@cornell.edu).

Color versions of one or more of the figures in this paper are available online at http://ieeexplore.ieee.org

Digital Object Identifier 10.1109/JLT.2010.2048414

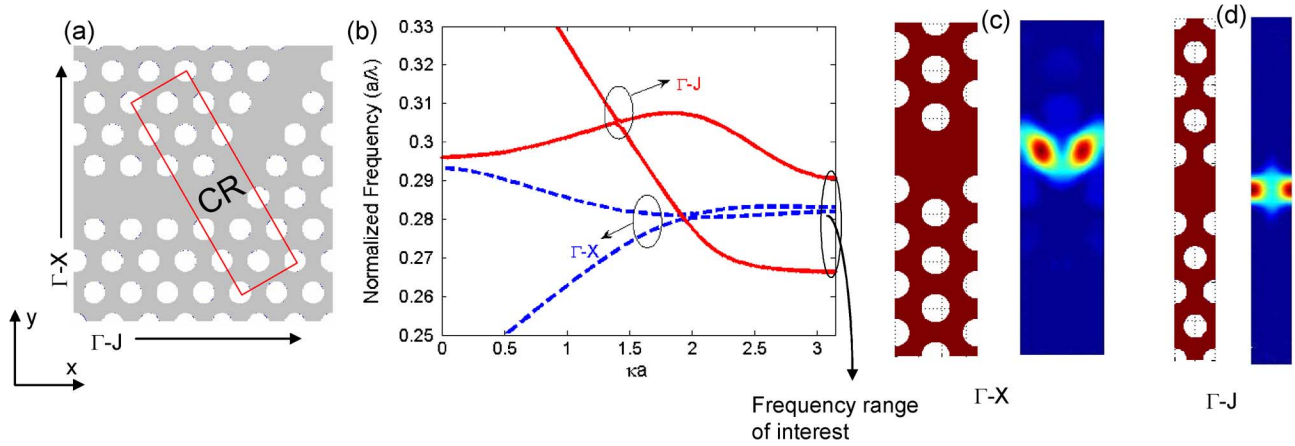

Fig. 1. (a) Simulation structure indicating the CR. (b) Dispersion diagram for Γ-J (solid) and Γ-X (dotted). (c) Unit cell and field profile (H_z) at $\omega_n = 0.27$ for the even-like mode for Γ-X (or CR) section. (d) Unit cell and field profile (H_z) at $\omega_n = 0.27$ for the even mode in the Γ-J section.

from the input waveguide (Γ-J section) into the PCW bend, CR, or Γ-X section, and then couples into the output waveguide (Γ-J section). To ensure good transmission over a large bandwidth, the guided modes within the two sections (i.e., the Γ-J and Γ-X) must be similar in terms of both the dispersion and the field profile of the modes. The dispersion provides information about the number of modes and the group velocity of the modes. When light—propagating in a single mode—couples from one section to another, the energy is distributed into the modes of the second section; hence, it is important that the second section is also single mode so that the energy is not coupled to unwanted modes. Similarly, the group velocity of the modes in the two sections should be similar to avoid reflections. The field profile, on the other hand, provides information about the distribution of the electromagnetic field along the guiding region. Since the tangential fields are continuous at an interface, it is important to match the field profiles of the two sections to avoid power reflection at the interface.

Fig. 1(a) shows a 2-D PCW bend in a triangular lattice PC of air holes (with radius r) in Si. To simplify the simulations, we have used the effective index model for Si $(\text{neff} = 2.811)$ to allow for 2-D analysis. The effective index is calculated using a 1-D mode solver [16]. The radius of air holes is $r = 0.3a\,(a = \text{lattice constant})$ to ensure maximum photonic bandgap for TM modes (i.e., modes with magnetic field perpendicular to the plane of periodicity). It is generally preferred to have two PCW bends to have parallel input and output waveguides. However, in our simulations we have used only one PCW bend to avoid the Fabry--Perot (FP) effect due to reflection between the bends. We have used 2-D finite difference time domain (2D-FDTD) [17] with incorporation of absorbing boundary conditions[1] to analyze the PCW bend transmission and dispersion characteristics.

For our simulations, lattice period (a) is equal to 24 FDTD grid points. To calculate the PCW bend power transmission spectrum in 2D-FDTD, we used a pulsed Huygens source [18] to excite the fundamental TM mode in the slab waveguide that is coupled to the simulation structure. The spectrum of the power transmitted through the bend is calculated by taking the Fourier transform of the fields and then integrating the Poynting vector over a surface of 161 grid points, centered at the middle of the output PCW. It is important to note that a point observation surface is not suitable for recording fields in a PCW waveguide as the TM profile changes a lot going from a high-group velocity mode to a low-group velocity mode. The power transmission spectrum is then calculated as the ratio of the power transmitted through the bend to the power transmitted through a similar PCW structure of equal length but with no bends. This allows us to remove the effect of coupling from the slab waveguide to the PCW.

For calculating the band structure and field profile of the modes in the two sections, we have used the plane-wave expansion method [19] with super cell technique. To further reduce the computation cost we have employed the effective index approximation to simplify the problem from 3-D to 2-D. The effective index used in our calculation is the same as the one used in our 2D-FDTD calculations.

III. Bend Design and Discussion

The dispersion diagrams of the guided modes of the two sections (Γ-J and Γ-X) are shown in Fig. 1(b). In this paper, we concentrate on the single-mode-normalized frequency region for the Γ-J waveguide $0.266 < \omega_n < 0.291$, eclipsed in Fig. 1(b). This range of frequencies is of most interest for integrated optics applications. Fig. 1(b) shows that the Γ-J section has a single mode in the frequency range of interest, whereas Γ-X section has two modes. It is also evident from Fig. 1(b) that the modal dispersion of the two sections are different in the frequency range $0.266 < \omega_n < 0.272$; the Γ-J section has low group velocities, whereas Γ-X section has large group velocities. Fig. 1(c) and (d) shows the intensity profile for the out-of-plane (or z) component of the magnetic field of the even and even-like mode in the Γ-J and Γ-X sections, respectively. Here, we are using the terms even-like and odd-like for the modes in the Γ-X section, because they have similar field profiles to even and odd modes of the Γ-J waveguide, but they cannot be termed as even/odd in the Γ-X section as it lacks mirror symmetry. The location of the intensity maximum within

[1]Special absorbing boundary conditions are required to absorb dispersive waves. We have used an in house developed absorbing boundary condition, which will be reported elsewhere.

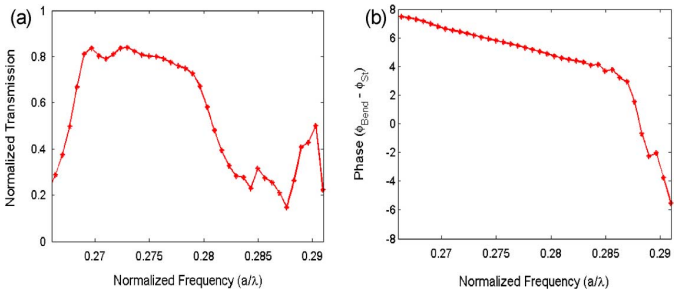

Fig. 2. (a) Transmission and (b) phase of the simple bend, structure shown in Fig. 1(a) with $r/a = 0.3$. The transmission and phase through the bend is normalized to those through a straight PCW with similar length.

the unit cell is different for the two sections; it is concentrated at the edge of the unit cell of the Γ-J waveguide along the *x* axis [see Fig. 1(d)], whereas it is shifted toward the center of the unit cell for the Γ-X waveguide [see Fig. 1(c)]. Since the tangential component of the magnetic field is continuous at an interface, it is expected that the difference in the intensity profiles of the two sections would result in unwanted reflections. Fig. 2(a) and (b), respectively, show the transmission and phase response of the simple bend structure, as shown in Fig. 1(a). The phase accumulated by the pulse in going through the bend section is calculated by subtracting the phase of the output pulse through the bend simulation from the phase of the output pulse through the straight PCW simulation. The total length of the PCW is kept the same in the two simulations, which allows us to extract the phase that the pulse accumulates while passing through the bend section. The differences in the dispersion and field profile of the two sections [i.e., Γ-X and Γ-J in Fig. 1(d)], as noted earlier, reflect as an overall reduction of transmission and the presence of low transmission regions at the lower and upper ends of the single-mode frequency range, as shown in Fig. 2(a). The phase response also shows strong dispersive behavior in the upper end of the frequency range of interest [see Fig. 2(b)].

Fig. 1(c) shows that the electromagnetic energy in the bend section is mainly concentrated in the middle of the waveguide region. Therefore, it is expected that the holes in the vicinity of the center of the waveguide region would have the maximum effect on the transmission and phase response of the bend. Thus, our design approach is to optimize the bend section, to achieve a better transmission and phase response, by engineering the size of the air holes that are in vicinity of the maximum field region. We identify five holes in this region and represent them by their radii, as shown in Fig. 3(a). We first study the effect of individual holes on the dispersion and the field profile of the coupling section.

The air hole identified as r_1, as shown in Fig. 3(a), is close to the center of the Γ-X guiding section of the bend. The effect of increasing r_1 on the dispersion of the guided modes of the Γ-X section is shown in Fig. 3(b). As r_1 is increased, the Γ-X dispersion moves to higher frequencies. This can be used to make the coupling section single mode in the frequency range of interest, by moving the range of frequencies in which Γ-X has two guided modes out of the frequency range of interest [i.e., the single mode region of the Γ-J section, as shown in Fig. 1(b)]. Since the even-like mode is more concentrated in the center of the guiding region as compared to the odd-like mode, the effect of increasing r_1 is more pronounced for the even-like mode. Increasing r_1 moves the even-like mode up in frequency more than the odd-like mode, causing a decrease in the single-mode bandwidth of the even-like mode of the Γ-X section. The effect of increasing r_1 on the field profile of the even-like mode of the Γ-X section, as shown in Fig. 3(c) and (d), is twofold. The field profile moves outward toward the edges of the unit cell of the coupling section. Thus, it provides a better match to the field profile of the even mode of the Γ-J section. It also moves the field profile upward (i.e., toward the inside of the bend); thus, it helps the electromagnetic energy to bend inward. The aforementioned discussion illustrates the effect of increasing r_1 on the dispersion and the field profile of the Γ-X section. However, hole radius r_1 cannot be increased beyond a value of $r_1/\mathrm{a} = 0.25$ (if this was the only hole radius we were changing) as above this value of r_1/a the lower frequency edge of the even-like mode dispersion of Γ-X section moves above the lower frequency edge of the even mode of the Γ-J section. In order to compensate for this, we have to reduce another air hole radius to bring the Γ-X dispersion down. This is achieved by reducing hole radius r_2, which causes the dispersion diagram to move down, and the field profile of the Γ-X section to move up toward the inside of the bend region. Decreasing r_2 also decreases the tilt in the field profile maximum causing it to look a lot more vertical (i.e., similar to the field profile of the mode in the Γ-J section). These effects of changing r_2 are easily predicted by considering its location within the Γ-X unit cell and the effect of r_1 on the dispersion and field profile. For example, if we reduce the value of r_2/a to 0.25 from its original value of 0.3 in a simple bend, the value of hole radius r_1/a can be increased to 0.31 without the low frequency edge of the even-like mode of the Γ-X dispersion moving above the low frequency edge of the even mode of the Γ-J dispersion.

The effect of increasing the size of r_e in Fig. 3(a) is shown in Fig. 4. Fig. 4(a) shows that the dispersion diagram of the even-like mode of the Γ-X section moves up at larger r_e similar to what is observed for increasing r_1. On the other hand, since the r_e holes are at the edges of the guiding region, the odd-like mode is more sensitive to its change than the even-like mode. As a result the odd-like mode moves up more than the even-like mode, as shown in Fig. 4(a). This increases the bandwidth of the single mode region with only even-like mode as the guided mode. By increasing r_e/a from 0.3 to 0.4, the odd-like mode moves out of the frequency range of interest at the higher frequency end. At the same time, increasing r_e pushes the field profile upwards (i.e., toward the inner corner of the bend) and helps bending the electromagnetic energy.

The primary effect of changing r_1, r_2, and r_e on the dispersion diagram is to move it up or down, and it has a minimal effect on its shape or slope. The slope of the dispersion, however, can be changed by modifying the holes that are not in the immediate vicinity of the guiding region [e.g., $\mathrm{r_o}$ in Fig. 3(a)]. Fig. 5(a) compares two Γ-X dispersions with the Γ-J dispersion (dotted curve). The two Γ-X dispersions, one with $r_\mathrm{o} = 0.37a$ (solid curve) and the other with $r_\mathrm{o} = 0.38a$ (dashed curve), lie on top of one another for most of the frequency range of interest. The other hole radii ($r_1 = 0.28a, r_2 = 0.25a$, and $r_e = 0.4\mathrm{a}$)

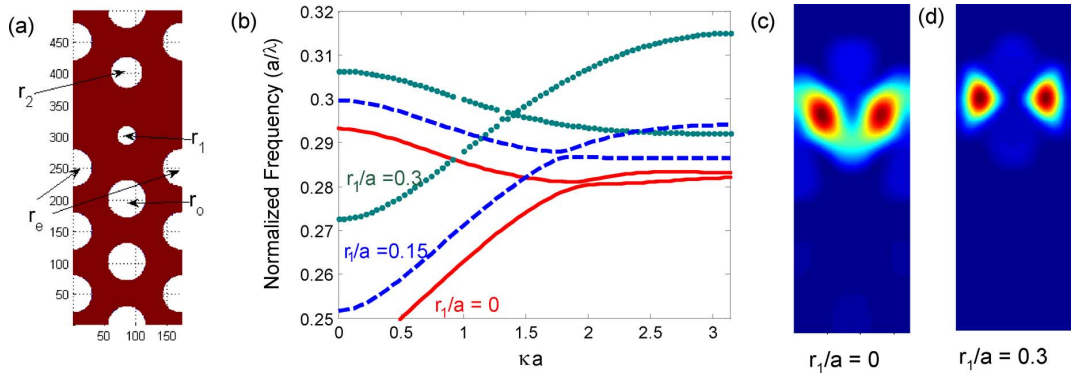

Fig. 3. (a) Important air holes for control of dispersion and field profile in a PCW bend. (b) Γ-X waveguide dispersion as a function of r_1/a with $r_1/a = 0.0$ (solid), $r_1/a = 0.15$ (dashed), and $r_1/a = 0.3$ (dotted). (c) Field profile of the even-like guided mode in the Γ-X region with (c) $r_1/a = 0.0$ and (d) $r_1/a = 0.3$. The size of all other holes is the same $(r/a = 0.3)$.

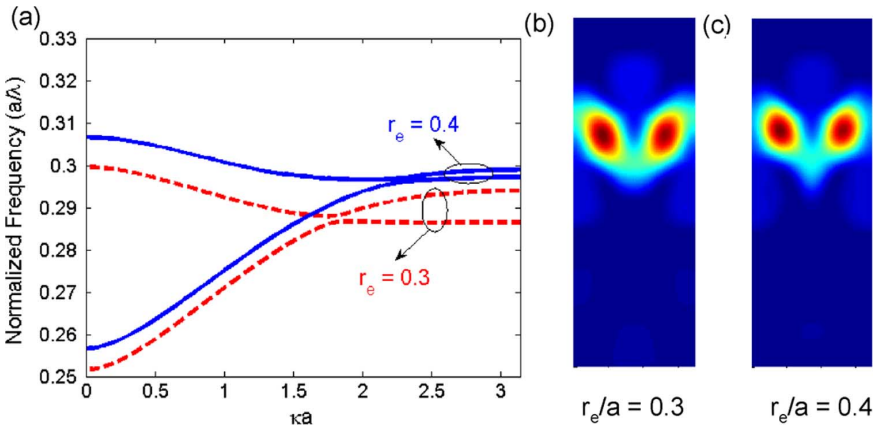

Fig. 4. (a) Effect of increasing r_e in Fig. 3(a), on dispersion diagram of the Γ-X section. The field profiles of the even-like mode for (b) $r_e/a = 0.3$ and (c) $r_e/a = 0.4$ (c). For these figures $r_1/a = 0.15$ and all the other hole radii are of value $r/a = 0.3$.

are the same for these two dispersions. These two dispersions differ only at the low frequency end $(\kappa a < 0.2)$, in which the dashed curve with a larger value of r_o is flatter. As we increase r_o, the dispersion of the mode that lies below the even-like mode (not shown in figure for clarity purpose) moves up in frequency and couples with the even-like mode. This coupling causes the even-like mode to flatten. The air hole r_o cannot be increased beyond the value of $0.38a$, as beyond this value the mode that lies below the even-like mode, moves into the frequency range of interest. Fig. 5(a), also shows the dispersion of the Γ-J even mode (dotted curve), which suggests that the flatter the even-like mode of the Γ-X coupling section, the more it resembles the Γ-J even mode dispersion. This would result in a better group velocity match over a larger range of propagation constant (κ) or frequency.

To further assist the electromagnetic energy to bend, we also use the interface between the Γ-J incident section and the Γ-X coupling section [see Fig. 5(b) and (c)]. The effect of increasing the radius of interface hole on the field pattern of the Γ-J even mode is shown in Fig. 5(d) and (e). Increasing the radius of interface air hole (r_{int}), at the upper edge of the interface, tilts the field profile inward, thus helping the electromagnetic energy to bend.

The effect of changing the location of the center of air holes such as r_1, r_2, and r_o on the transmission and phase behavior of bends was also studied. Our simulations indicate that this change in location of air holes improves the transmission and phase response at large group velocities at the expense of transmission and phase response at low group velocities. Since our focus has been mostly on the low-group velocity region, we do not consider changing the hole locations in our systematic design and optimization.

The main point of the earlier discussion is that each hole in the vicinity of the guiding region affects both the dispersion and the field profile of the mode in the Γ-X section. Thus, any optimal design needs to take into account the coupled effect of all the air holes on both the dispersion and the field profile. The effect of individual air holes on the dispersion and field profile is mentioned in Table I.

Having studied the effects of individual air holes on the dispersion and field profile, we turn our attention to the systematic design. First, the air hole r_e is increased to $0.4a$, this pushes the odd-like mode up in frequency and increases the single mode guiding bandwidth of the even-like mode of the Γ-X bend section. It also moves the field profile up toward the inside of the bend (see Fig. 4 for the effects of increasing r_e on the dispersion).

The air holes r_1 and r_2 are then used to align the lower frequency end of the Γ-X even-like mode dispersion to the lower frequency end of the Γ-J even mode dispersion. This can be

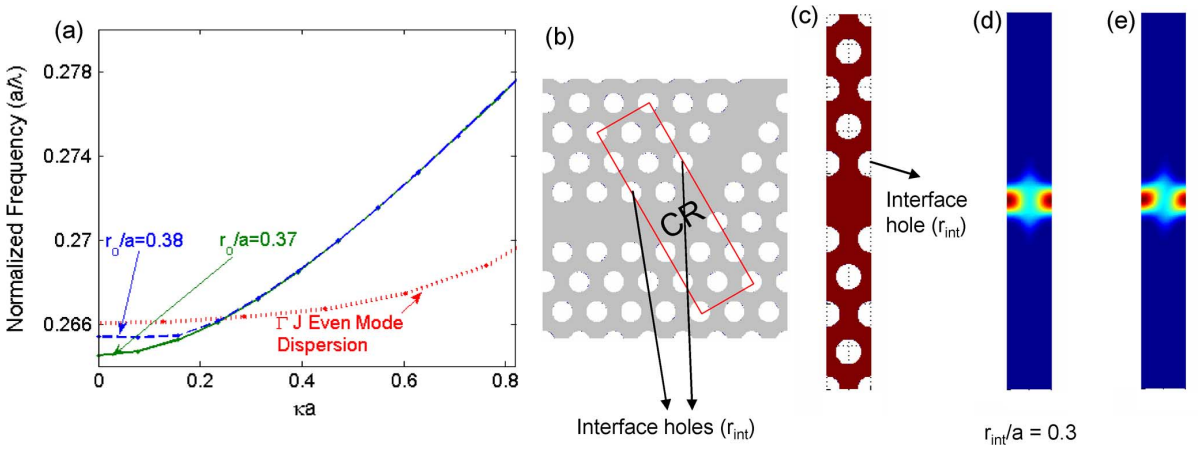

Fig. 5. (a) Γ-X dispersion for different air hole radius r_o/a with other hole radii constant at $r_1 = 0.28a, r_2 = 0.25a, r_e = 0.4a$. The dispersion diagram of the structure with $r_o = 0.38a$ (dashed curve) is flatter than that for the structure with $r_o = 0.37a$ (solid curve). The dispersion of the even mode in the Γ-J section with $r/a = 0.3$ is shown for comparison (dotted curve). Location of interface holes in (b) bend and (c) Γ-J unit cell. Field profiles for (d) $r_{\rm int}/a = 0.3$ and (e) $r_{\rm int}/a = 0.35$.

TABLE I
EFFECT OF INDIVIDUAL AIR HOLES ON DISPERSION AND FIELD PROFILE

AIR HOLES	EFFECT ON EVEN-TYPE MODE DISPERSION	EFFECT ON ODD-TYPE MODE DISPERSION	EFFECT ON FIELD PROFILE
r_1	Major	Minor	Major
r_2	Major	Minor	Major
r_e	Minor	Major	Minor
r_o	Major (only at low group velocities and negligible otherwise)	Negligible	Negligible

achieved for different combinations of r_1 and r_2 (e.g., $r_1 = 0.29a$ and $r_2 = 0.25a; r_1 = 0.32a$ and $r_2 = 0.22$a; and $r_1 = 0.35a$ and $r_2 = 0.19a$) as the Γ-X even-like mode dispersion is equally sensitive to both r_1 and r_2. Our simulations show that the transmission and the phase response for all of the aforementioned combinations of r_1 and r_2 are very similar with only minor variations in the transmission or phase in the frequency range of interest. Emphasizing more on the transmission at small group velocities, the best bend performance is obtained for $r_1 = 0.35a, r_2 = 0.19a, r_e = 0.4a$, and $r_o = 0.38a$ due to the better field profile match of the modes of the two sections (Γ-J and Γ-X) at small group velocities. The value of 0.38 is chosen for r_o/a as it allows a better group velocity match for the even-like mode of Γ-X section to the small group velocity modes of the Γ-J section.

The aforementioned values of hole radii are an optimum within the parameter space explored in this study. Although this combination of hole radii may not represent the global optimum, it should provide an excellent starting point for more sophisticated optimization schemes (e.g., genetic algorithm) to obtain the global optimum.

The insensitivity of the transmission and phase response of our designed bends to different combinations of hole radii as mentioned earlier indicate a good tolerance of the structure to the change in size of air holes that might happen during fabrication. We also studied the sensitivity of the bend performance to changes in hole radii to within a couple of percent of the optimized bend hole radii, as can be expected in fabrication. It was found that this random change in hole sizes results in only minor changes in transmission and phase response, and hence, the designed bends have good tolerance to fabrication variations.

In Fig. 6, we compare the performance of our optimized bend design with that of a simple bend (with no modification to the holes in the vicinity of the guiding region). Fig. 6(a) shows that our design has higher transmission at both the high and low frequency ends of the single mode region $(0.266 < \omega_n < 0.291)$, which, respectively, correspond to fast and slow group velocity range of operation for the PCW bends. The 3 dB bandwidth of our design is almost twice that in the simple bend, and it now covers the entire single-mode guiding region of the input and output PCW. Fig. 6(b) compares the phase response of our bend design with a simple bend. The phase response of our design is almost linear throughout the frequency range of interest. Thus, the dispersion introduced by our design would be negligible as compared to that introduced by the simple bend. The main advantages of our design as compared to a simple bend are that it has high transmission and negligible dispersion throughout the frequency range of interest.

We are currently in the process of fabricating our bends and the experimental results will be reported elsewhere. Although we have not used 3-D simulations in designing our bends to account for out-of-plane losses, we do not expect these losses to be high, similar to the earlier report on the comparison of bend performance calculated using 2D-FDTD and 3D-FDTD [14]. Also, it has been shown experimentally [22] that the bending loss due to light leakage is less than 0.08 dB, which justifies the use of 2D-FDTD simulations.

IV. COMPARISON WITH OTHER REPORTED BEND DESIGNS

In this section, we compare the results of our bend design with other bend designs reported in literature. Benisty *et al.* [20] have treated the bend as a mode scrambler. They move the holes from the inner corner of the bend to the outer corner to convert the bend section from a single 60° section to two 30° sections. For fair comparison, we simulated the design in [20], using our simulation platform and the results of the mode

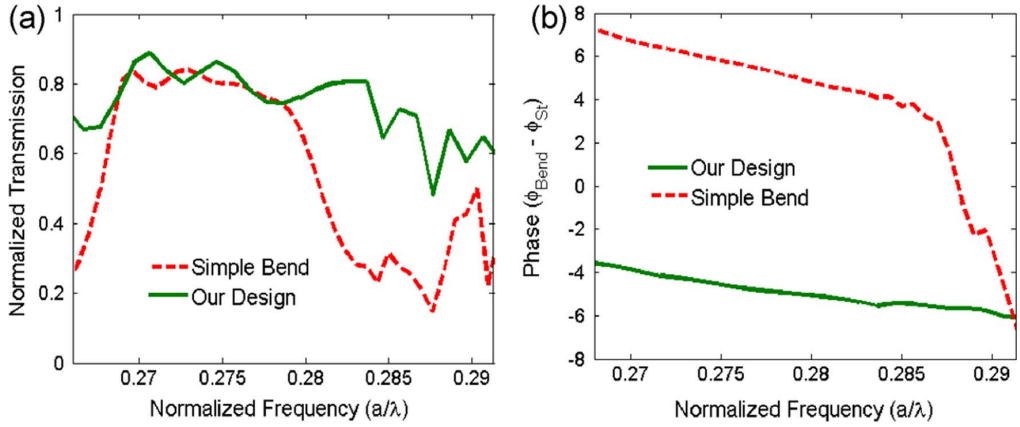

Fig. 6. Comparison of (a) normalized transmission and (b) phase of our bend design with $r_1 = 0.35a, r_2 = 0.19a, r_e = 0.4a$, and $r_o = 0.38a$ (solid curve) with a simple bend with $r_1 = 0, r_2 = 0.3a, r_e = 0.3a$, and $r_o = 0.3a$ (red-dashed curve) design. The PC is triangular lattice of air holes in Si. For all other air holes $r/a = 0.3$.

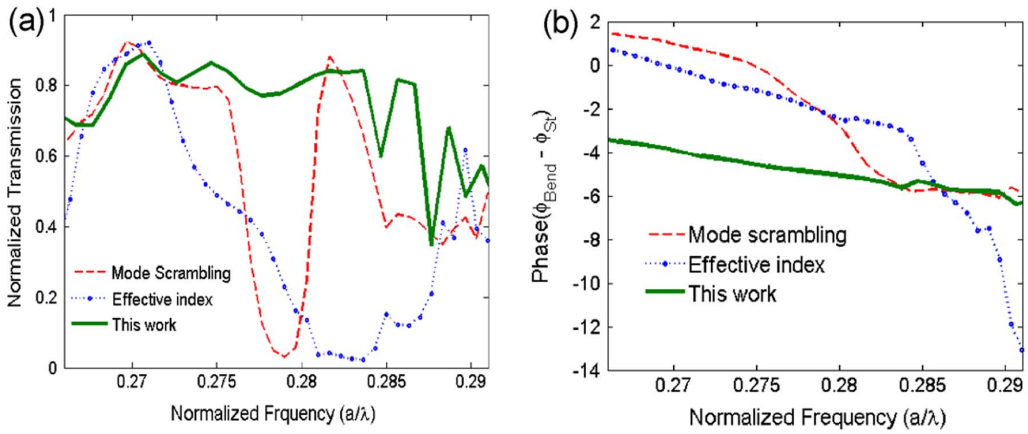

Fig. 7. Comparison of (a) normalized transmission and (b) phase of our design (solid curve) with bends designed, using the mode scrambling technique [20] (dashed curve) design and that using the effective index matching technique [21] (dotted curve).

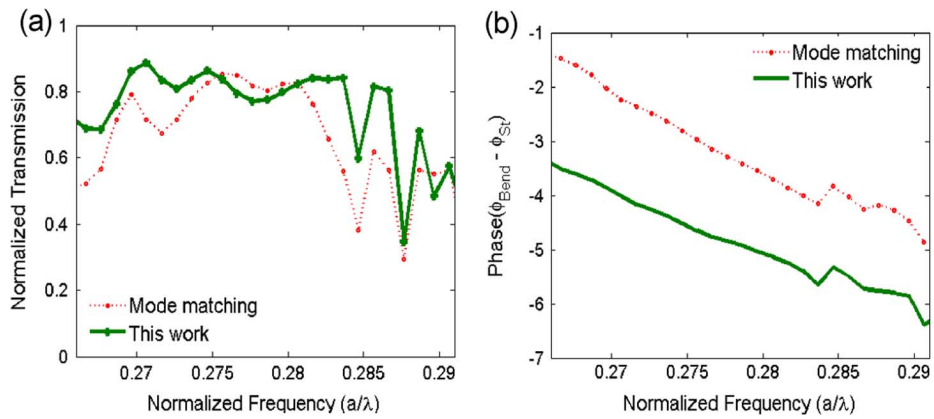

Fig. 8. Comparison of (a) normalized transmission and (b) phase of the bend designed in this paper (solid curve) with those of the bend designed by mode matching [14] (dotted curve) design.

scrambling technique (dashed curve) are compared with our design (solid curve) in Fig. 7. From the transmission comparison [see Fig. 7(a)], our design works better for most of the single mode frequency range. Only for a small range of frequencies around $\omega_n = 0.27$ does the bend designed, using the mode scrambling technique performs better. However, this bend has very low transmission in the frequency range $(a/\lambda)0.277 < \omega_n < 0.281$. The phase response, as shown in Fig. 7(b), of our design is considerably more linear than that of the mode scrambling technique of [20], and hence, it is less dispersive for the optical pulse propagating through it. Fig. 7 also compares the performance of our bends (solid curve) with that of bends designed in [21] (dotted curve), simulated using our platform. In [21], Moll and Bona reduce the size of the holes in the

vicinity of the bend section to match the effective index that the mode encounters in the bend section to what it encounters in the straight waveguide section.

From the transmission comparison in Fig. 7(a), it is obvious that although the effective index scheme works well over a small bandwidth in the low frequency range (for which the bend in [21] was designed), it results in a bend with low transmission for $\omega_n > 0.272$. Comparison of the phase response also shows that our design is less dispersive than the design reported in [21].

Chutinan *et al.* [14] consider the bend section as a Γ-X waveguide section, similar to what we used in this paper. A simple bend has two modes, as shown in Fig. 1(d). In [14], the bend section is made single mode by adding holes in the center of the waveguide. In Fig. 8, we compare the transmission and phase response of the bend designed in [14] (dotted curve), simulated using our platform, and our bend (solid curve). The shape of the transmission curve in the two cases is reasonably similar, but the transmission amplitude for our bend is better in most of the frequency range of interest, especially at small group velocities. The phase response of the two designs is very similar as well. Also, since the design reported in [14] consists of four additional air holes per bend in the guiding region than our design, it would likely result in higher out-of-plane scattering losses.

V. Conclusion

The results presented in this paper clearly show that a PCW bend can be modeled as a coupling section between Γ-J directed input and output waveguides. We showed that by matching the dispersion and field profile of the Γ-J guiding regions and the Γ-X bend region in a triangular lattice PCW, we can achieve both high-transmission and linear phase response for the bend in the entire frequency range of interest. This design is achieved by systematically modifying the size of only four air holes in the vicinity of the guiding region in the bend. We also compared the transmission and phase response of our bends with other results reported in literature and showed that our design provides better characteristics. Although we applied our approach to the triangular lattice PCWs, it is quite general and can be extended to any PC lattice.

References

[1] E. Yablonovitch, "Inhibited spontaneous emission in solid state physics and electronics," *Phys. Rev. Lett.*, vol. 58, pp. 2059–2062, May 1987.

[2] S. John, "Strong localization of photons in certain disordered dielectric superlattices," *Phys. Rev. Lett.*, vol. 58, pp. 2486–2489, Jun. 1987.

[3] A. Mekis, S. Fan, and J. D. Joannopoulos, "Bound states in photonic crystal waveguides and waveguide bends," *Phys. Rev. B*, vol. 58, pp. 4809–4817, Aug. 1998.

[4] A. Adibi, Y. Xu, R. K. Lee, A. Yaariv, and A. Sherrer, "Properties of slab modes in photonic crystal optical waveguides," *J. Lightw. Technol.*, vol. 18, no. 11, pp. 1554–1564, Nov. 2000.

[5] M. Notomi, K. Yamada, A. Shinya, J. Takahashi, C. Takahashi, and I. Yokohoma, "Extremely large group-velocity dispersion of line-defect waveguides in photonic crystal slabs," *Phy. Rev. Lett.*, vol. 87, pp. 253902-1–253902-4, Dec. 2001.

[6] H. Gersen, "Real-space observation of ultraslow light in photonic crystal waveguides," *Phy. Rev. Lett.*, vol. 94, pp. 073903-1–073903-4, Feb. 2005.

[7] J. Li, T. P. White, L. O'Faolain, A. Gomez-Iglesias, and T. F. Krauss, "Systematic design of flat band slow light in photonic crystal waveguides," *Opt. Exp.*, vol. 16, pp. 6227–6232, 2008.

[8] Y. Hamachi, S. Kubo, and T. Baba, "Slow light with low dispersion and nonlinear enhancement in a lattice-shifted photonic crystal waveguide," *Opt. Lett.*, vol. 34, pp. 1072–1074, 2009.

[9] J. McMillan, X. Yang, N. Panoiu, R. Osgood, and C. Wong, "Enhanced stimulated Raman scattering in slow-light photonic crystal waveguides," *Opt. Lett.*, vol. 31, pp. 1235–1237, 2006.

[10] L. Gu, W. Jiang, X. Chen, and R. Chen, "Thermooptically tuned photonic crystal waveguide silicon-on-insulator Mach–Zehnder interferometers," *IEEE Photon. Technol. Lett.*, vol. 19, no. 5, pp. 342–344, Mar. 2007.

[11] A. Mekis, J. C. Chen, I. Kurland, S. Fan, P. R. Villeneuve, and J. D. Joannopoulos, "High transmission through sharp bends in photonic crystal waveguides," *Phys. Rev. Lett.*, vol. 77, pp. 3787–3790, Oct. 1996.

[12] S. Boscolo, C. Conti, M. Midrio, and C. G. Someda, "Numerical analysis of propagation and impedance matching in 2-D photonic crystal waveguides with finite length," *J. Lightw. Technol.*, vol. 20, no. 2, pp. 304–310, Feb. 2002.

[13] M.-F. Lu, Y.-L. Yang, and Y.-T. Huang, "Numerical study of transmission improvement in a photonic crystal waveguide bend by mode-matching technique," *IEEE Photon. Technol. Lett.*, vol. 20, no. 24, pp. 2114–2116, Dec. 2008.

[14] A. Chutinan, M. Okano, and S. Noda, "Wider bandwidth with high transmission through waveguide bends in two-dimensional photonic crystal slabs," *Appl. Phys. Lett.*, vol. 80, pp. 1698–1700, Mar. 2002.

[15] S. Blair and J. Goeckeritz, "Effect of vertical mode matching on defect resonances in one-dimensional photonic crystal slabs," *J. Lightw. Technol.*, vol. 24, no. 3, pp. 1456–1461, Mar. 2006.

[16] R. Pollock, *Fundamentals of Optoelectronics*. Homewood, IL: Irwin, 1995.

[17] K. S. Yee, "Numerical solution of initial boundary value problems involving Maxwell's equations in isotropic media," *IEEE Trans. Anntennas Propag.*, vol. AP-14, no. 3, pp. 302–307, May 1966.

[18] D. E. Merewether, R. Fisher, and F. W. Smith, "On implementing a numeric Huygen's source scheme in a finite difference program to illuminate scattering bodies," *IEEE Trans. Nucl. Sci.*, vol. NS-27, no. 6, pp. 1829–1833, Dec. 1980.

[19] J. D. Joannopoulos, R. D. Meade, and J. N. Winn, *Photonic Crystals*. Princeton, NJ: Princeton Univ. Press, 1995.

[20] H. Benisty, "Models and measurements for the transmission of submicron-width waveguide bends defined in two-dimensional photonic crystals," *IEEE J. Quantum Electron.*, vol. 38, no. 7, pp. 770–785, Jul. 2002.

[21] N. Moll and G. L. Bona, "Bend design for low-group-velocity mode in photonic-crystal waveguides," *Appl. Phys. Lett.*, vol. 85, pp. 4322–4324, 2004.

[22] S. Assefa, S. J. McNab, and Y. A. Vlasov, "Transmission of slow light through photonic crystal waveguide bends," *Opt. Lett.*, vol. 31, pp. 745–747, 2006.

Author biographies not included at authors' request due to space constraints.